CARBON 79 (2014) 442–449

Available at www.sciencedirect.com

ScienceDirect

journal homepage: www.elsevier.com/locate/carbon

Stable hierarchical superhydrophobic surfaces based on vertically aligned carbon nanotube forests modified with conformal silicone coating

Dong-Wook Jeong [a,1], Ung-Hui Shin [b,1], Ji Hoon Kim [a], Soo-Hyung Kim [a,b,c], Hyung Woo Lee [a,d,*], Jong-Man Kim [a,b,c,*]

[a] Department of Nano Fusion Technology, Pusan National University, Busan 609-735, Republic of Korea
[b] Department of Advanced Circuit Interconnection, Pusan National University, Busan 609-735, Republic of Korea
[c] Department of Nanomechatronics Engineering, Pusan National University, Busan 609-735, Republic of Korea
[d] Department of Nanomaterials Engineering, Pusan National University, Busan 609-735, Republic of Korea

ARTICLE INFO

Article history:
Received 2 June 2014
Accepted 1 August 2014
Available online 11 August 2014

ABSTRACT

Unique and inherent nano-roughened morphologies of vertically aligned carbon nanotube (VACNT) forests are desirable for mimicking biological superhydrophobic surface systems. In this paper, we report on a new class of robust dual-roughened superhydrophobic surfaces based on VACNT forests coated conformally with thin silicone. The vapor phase deposition of silicone considerably reduces the surface energy of the VACNTs by conformally and completely covering the vertical structures. This significantly enhances the superhydrophobic robustness of the VACNTs by preventing the surfaces from being wet, even under pressurized conditions. In addition, micro-patterning based on a simple contact transfer technique enables easy fabrication of VACNT micro-pillar arrays with various pillar-to-pillar spacings ranging from 45 to 160 μm with respect to a fixed width of ~65 μm. A combination of simple contact transfer and subsequent silicone coating techniques facilitates the achievement of micro/nano hierarchical VACNT superhydrophobic surfaces with superior wetting properties (high water contact angle of 168 ± 0.3°, low contact angle hysteresis of 2.64 ± 0.4°, and low sliding angle of <~5°) and water-repellent performance (even at impact velocity of up to ~1.4 m/s) while ensuring superhydrophobic robustness.

1. Introduction

Over the past decades, superhydrophobic surfaces have attracted great attention due to their potential in practical applications, which is facilitated by their unique and desirable properties such as self-cleaning and water-repellency [1–5]. In general, the wetting properties of such solid surfaces strongly depend on the chemical composition and geometrical features of the surfaces. In particular, the surface roughness plays a very important role in achieving non-wetting surfaces with enhanced superhydrophobic properties that ensure a water contact angle (WCA) larger than 150° and a contact angle hysteresis (CAH) smaller than 10°. A number of different material systems have been used to demonstrate

* *Corresponding authors at:* Department of Nano Fusion Technology, Pusan National University, Busan 609-735, Republic of Korea. Fax: +82 51 514 2358 (H.W. Lee), +82 55 350 5289 (J.-M. Kim).
E-mail addresses: lhw2010@pusan.ac.kr (H.W. Lee), jongkim@pusan.ac.kr (J.-M. Kim).
[1] These authors contributed equally to this work.
http://dx.doi.org/10.1016/j.carbon.2014.08.002
0008-6223/

functional superhydrophobic surfaces by creating multiscale roughness on the surfaces with various fabrication techniques [2–7].

Recently, vertically aligned carbon nanotube (VACNT) forests have been considered as one of the most straightforward approaches to mimic nature's non-wetting surface designs owing to the fairly uniform nanoscale surface roughness on their vertical architectures [8–13,18–25]. However, it is well-known that droplets on VACNT forests are typically not stable because they can eventually seep into the inter-CNT spaces on the surfaces within a few minutes after introduction [8,9]. Moreover, the surface morphologies of VACNT forests with uniformly and densely packed CNTs can be irreversibly deformed by the surface-tension-driven bundling of adjacent CNTs during drying [9]. Therefore, versatile surface functionalization methods have also been developed to improve the superhydrophobic robustness of VACNT forests [8–13].

Recent studies have verified theoretically and experimentally that hydrophobic performance can be significantly enhanced on hierarchically structured surfaces [14,15]. Therefore, a number of fabrication approaches have been developed to create dual-scaled hierarchical surface geometries including plasma etching, chemical reactions, self-assembly, hydrothermal treatment, spin-coating, and electrodeposition [16–24]. In addition, many attempts have been made to demonstrate hierarchical VACNT forests by combining microscale structures with the inherent nanoscale surface roughness of VACNT forests [25–32]. Some groups have fabricated double-roughened superhydrophobic surfaces by growing aligned CNTs entirely on micro-patterned silicon templates deposited with catalytic metal layers [18–20]. Although the resultant hierarchical surfaces clearly showed enhanced wetting properties compared to those of mono-scale ones, the fabrication complexity may be unavoidable due to the multi-step processes for preparing the micro-pillar-arrayed silicon templates.

In addition, many have reported enhanced hydrophobicity of VACNT forests by three-dimensionally structuring them through a site-selective growth on catalyst patterns prepared by various approaches, including photolithography [27,28], nanosphere lithography [29], pattern transfer [30]. These methods would be preferable to alleviate the complexity in the fabrication of dual-scale VACNT forests. However, it would be quite a challenge to prepare arbitrary shapes of VACNT patterns uniformly on a large area because of the catalyst geometry-dependent growth behavior of VACNTs [31]. As a top-down approach, a laser pruning technique has been used to create hierarchical VACNT microwalls with improved hydrophobicity [32]. Although VACNT microwalls with various widths could be periodically fabricated using a focused laser beam system, complex and highly controllable equipment is inevitably required for micropatterning VACNT forests.

In this work, stable hierarchical superhydrophobic surfaces based on VACNT micro-pillar arrays with inherent nanoscale roughness are fabricated and characterized. The superhydrophobic robustness of VACNT forests is simply achieved through a conformal and complete coating of thin hydrophobic silicone layer using a simple vapor phase deposition. The VACNT micro-pillar arrays with different inter-pillar spaces are easily fabricated in a designable manner by selectively removing unnecessary portions of VACNT forests through a simple contact transfer technique. This makes it possible to simply demonstrate dual-scale hierarchical VACNT surfaces with microscale roughness (micro-pillar arrays) and nanoscale roughness (nano-asperities on the VACNT micro-pillar surfaces), resulting in the enhancement of superhydrophobicity in the Cassie-Baxter regime.

2. Experimental details

2.1. Synthesis of VACNT forest and conformal silicone coating

VACNT forests were synthesized on a silicon substrate with a ~300-nm-thick thermally grown silicon dioxide (SiO_2) layer using a thermal chemical vapor deposition (T-CVD) process. Prior to VACNT growth, electron-beam evaporation and atomic layer deposition (ALD) techniques were employed to deposit a ~2-nm-thick catalytic metal film (iron, Fe) and a ~10-nm-thick barrier layer (alumina, Al_2O_3) on the supporting silicon substrate. After placing the catalyst-deposited samples into a T-CVD reactor, the reactor was ramped to 625 °C and the temperature was held for 30 s to establish catalytic islands while maintaining a pressure of 80 mbar and a hydrogen (H_2) flow rate of 700 cubic centimeters per minute (sccm). Subsequently, ethyne (C_2H_2) gas was introduced to the reactor at 50 sccm as a precursor for the growth of VACNT forests while keeping the reactor at 80 mbar and 625 °C. The height of VACNT forests was easily determined by controlling the growth time.

A thin silicone layer was conformally coated on as-prepared VACNT forests to make the surfaces hydrophobic while maintaining nanoscale morphologies using a vapor phase deposition technique [33]. For this, the VACNT forest sample (3 cm × 6 cm) and a PDMS slab, which is employed as a coating source, were first placed in a beaker without overlapping each other, and the beaker was carefully covered with an aluminum foil. The covered beaker containing the sample and source was then placed in an electric furnace (MF 32-G, JEIO TECH), followed by heating to ~250 °C for 30 min to form a conformal silicone layer on the VACNT forests.

2.2. Fabrication of hierarchical VACNT superhydrophobic surfaces

Hierarchical VACNT structures were fabricated by forming VACNT micro-pillar arrays on surfaces using a simple contact transfer technique facilitated by a PDMS stamp with sticky surface. The PDMS stamp was fabricated by a standard soft-lithography process. For this, a negative-tone photoresist (PR; THB-151N, JSR Micro) was first spun on an oxidized silicon substrate at 700 rpm for 20 s using a spin-coating system and planarized at room temperature for 24 h. After soft baking at 120 °C for 20 min on a hotplate to evaporate the solvent, the PR layer was selectively exposed to an ultraviolet light source with a photomask using a photolithographic system. Finally, ~70-μm-thick PR molds

were prepared by developing non-crosslinked PR portions in a 2.38% tetramethylammonium hydroxide (TMAH) solution. PDMS prepolymer (Sylgard 184 A, Dow Corning) mixed with a curing agent (Sylgard 184 B, Dow Corning) at a weight ratio of 20:1 was poured onto the prepared PR molds after entirely removing air bubbles in a vacuum desiccator. Subsequently, the PDMS mixture was slightly polymerized at 70 °C for 15 min for easy manipulation while ensuring sticky surfaces, which are greatly desirable for easy patterning in the following contact transfer process.

After carefully peeling off from the PR mold substrate, a PDMS stamp was prepared and placed on the sample while facing the VACNT forest. The PDMS stamp was then pressed slightly to ensure conformal interfacial contact between the stamp and VACNTs while carefully monitoring the contact parts through the optically transparent PDMS stamp, followed by fully curing at 70 °C for 15 min to promote strong physical binding at the bonding interface. The square VACNT micro-pillar arrays were defined on the substrate by selectively removing the VACNT parts in contact with the stamp. Based on this approach, VACNT micro-pillar arrays with various pillar-to-pillar spacings ranging from 45 to 160 μm with respect to a fixed width of ~65 μm were easily fabricated. This simple strategy makes it possible to achieve the dual-scale VACNT surfaces with pillar-arrayed micro-roughness incorporated with inherent nanoscale CNT asperities. Finally, all the processed samples were conformally coated with a thin hydrophobic silicone layer.

2.3. *Characterization*

The morphologies of the as-prepared and micro-pillar-arrayed VACNT forests with thin silicone layers were characterized using filed-emission scanning electron microscopy (FESEM; S4700, Hitachi). Their chemical compositions were examined using energy dispersive X-ray spectroscopy (EDX), which is equipped with FESEM. The WCAs of the prepared samples were measured with 10-μL deionized (DI) water droplets by a sessile drop method using a commercially available contact angle meter (KRÜSS, DSA 20E) equipped with a CCD camera module. The CAHs were characterized by calculating the differences between the advancing and receding WCAs measured while continuously increasing (to 13 μL) and decreasing (to 7 μL) the volume of water droplets (initial 10 μL), respectively. All the measurements of WCAs and CAHs were carried out on at least five different regions.

For the squeezing test, a PDMS slab with a 10-μL water droplet was first placed on the prepared samples that were facing each other. After precisely leveling the stage, the droplet was squeezed on the surfaces of the VACNT forests by pressing the PDMS slab at a speed of ~1 mm/s and subsequently lifted while observing the surface states during the process.

For the sliding test, a 10 μL water droplet was gently introduced to the sample with the inter-pillar spacing of 160 μm after placement on a custom-made tilting stage equipped in the contact angle meter. The sliding behavior of the water droplets was examined by real-time observation using a

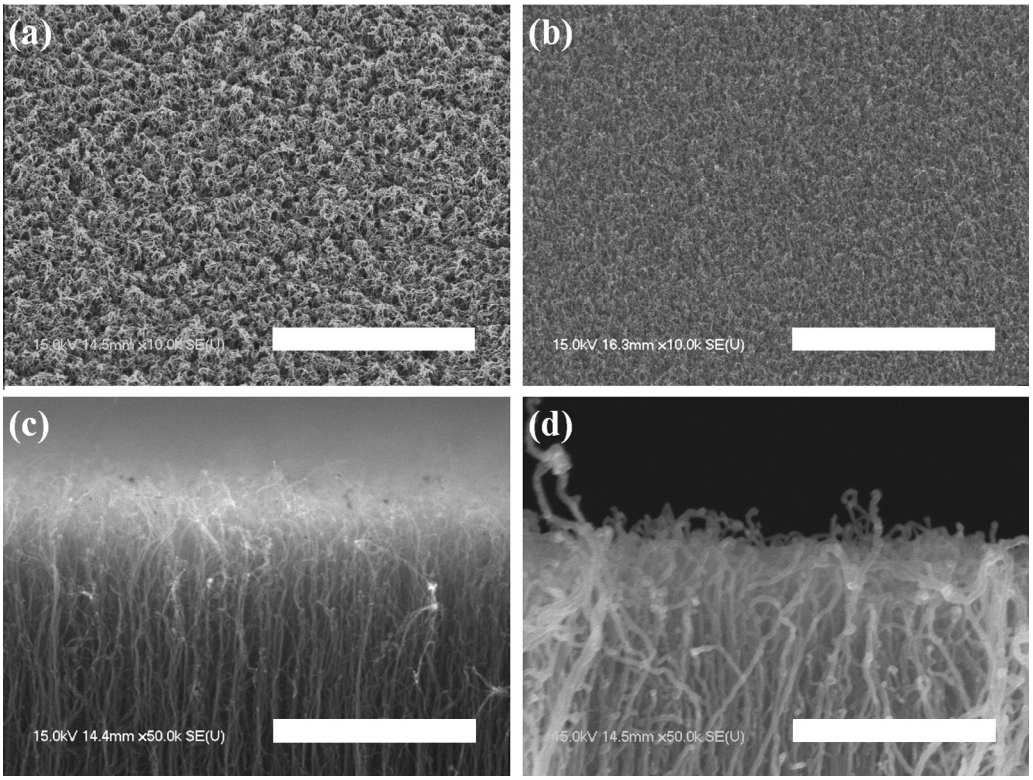

Fig. 1 – VACNT forests. Surface morphologies of (a) as-prepared and (b) silicone-coated VACNT forests (scale bars: 5 μm). Cross section profiles of (c) as-prepared and (d) silicone-coated VACNT forests (scale bars: 1 μm).

high-speed digital video camera (Photron, FASTCAM SA3) with a maximum frame rate of 120,000 frames/s.

For the impact test, a 10-μL water droplet was dropped on the sample with an inter-pillar spacing of 160 μm at various impact heights (H_I = 20, 40, 60, 80, and 100 mm) by a syringe installed in the contact angle meter. The resultant impinging-and-rebounding behaviors of the water droplets were observed carefully and recorded in real time using a high-speed digital video camera.

3. Results and discussion

Fig. 1(a) and (b) shows the surface morphologies of the as-prepared and silicone-coated VACNT forests, respectively. The SEM images indicate uniform nanoscale roughness on both surfaces. However, the magnified cross-sectional SEM image in Fig. 1(d) clearly shows that VACNTs at the surface regions are covered conformally with a thin silicone layer, in contrast to the as-prepared samples (Fig. 1(c)).

The presence of the conformal silicone layer was further proven by characterizing the cross sections of the silicone-coated VACNT forest using SEM and EDX analysis (Fig. S1 in Supporting Information). Prior to surface characterization of the silicone-coated VACNTs, the effect of the silicone layer on surface wetting properties was first examined by measuring and comparing the WCAs and CAHs of the bare and silicone-coated silicon surfaces. Consequently, the intrinsic WCA and CAH of the bare silicon surface were improved after silicone coating by ~84.5% and ~13.2%, respectively (Fig. S2 in Supporting Information). This means that the deposition of the thin silicone layer contributed greatly to making the solid surface hydrophobic by reducing the surface energy.

Fig. 2(a) shows the WCAs measured on the as-prepared and silicone-coated VACNT forests as a function of volume of the water droplet. In this case, the measurements were performed immediately after sitting the water droplets on the surfaces to avoid time-dependent changes of WCA on the as-prepared VACNT forest, as observed in Fig. S3 in Supporting Information. The WCA of the as-prepared VACNTs was gradually decreased while increasing the volume to 30 μL. This reveals that the surface state of the as-prepared VACNT forest is too unstable to be wet, even with the pressure increased slightly due to the increase in volume of the water droplet. Fig. 2(b) shows the surface morphology of the tested as-prepared VACNTs after fully evaporating the water components. It was seen that bundles of the VACNTs were formed probably due to the surface tension generated during drying [9], which also verifies that the water droplet eventually permeated into the spaces among the VACNTs.

On the other hand, the static wetting properties of the silicone-coated VACNTs were found to be stable while maintaining higher WCAs than those of the as-prepared ones regardless of the volume of the droplet (Fig. 2(a)). Even after drying, the nanoscale surface roughness was retained well without any appreciable morphological changes, as shown in Fig. 2(c).

This suggests that the thin silicone layer performs an important function in achieving stable superhydrophobic performance of the VACNT forests by facilitating the retention of

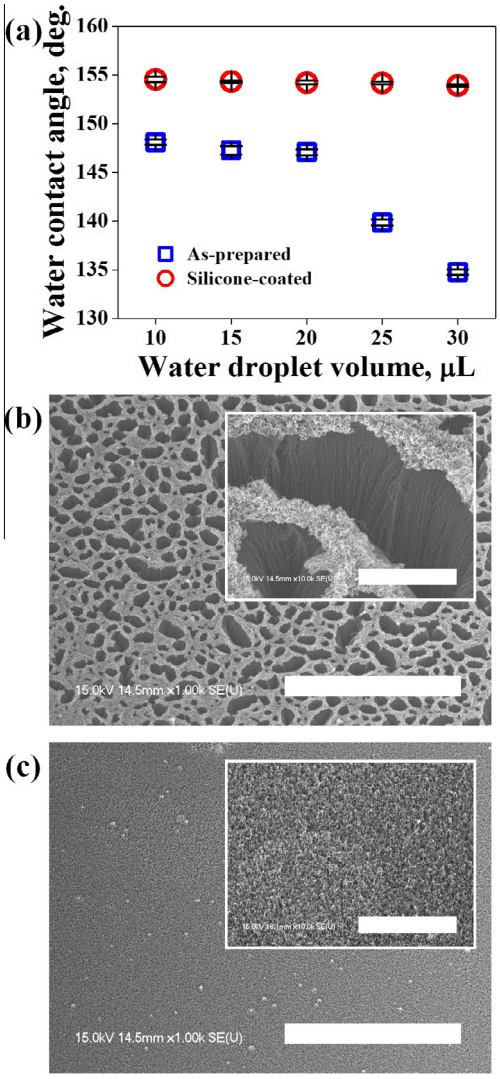

Fig. 2 – Superhydrophobic robustness of silicone-coated VACNT forests. (a) WCAs measured on the as-prepared and silicone-coated VACNT forests as a function of water droplet volume. Surface morphologies of the tested VACNT forests after fully evaporating water: (b) as-prepared, and (c) silicone-coated (scale bars: 50 μm) (insets: magnified views, scale bars: 5 μm). (A color version of this figure can be viewed online.)

the inherent nanoscale roughness of VACNTs (which have a large fraction of air in the surface) and protecting the forests from water penetration.

The superhydrophobic robustness of the samples was further examined by the squeezing test, as shown in Fig. 3. When the water droplet squeezed on the as-prepared VACNT surface was lifted, the droplet was severely deformed while bridging the two surfaces. Upon further lifting, the droplet was eventually separated while leaving some portion of the droplet with much lower WCA on the VACNT surface, as shown in Fig. 3(a). This probably originates from an increase in the interfacial contact area of water droplets to the CNT surfaces with relatively high surface energy due to water penetration into the spaces among the VACNTs. On the other

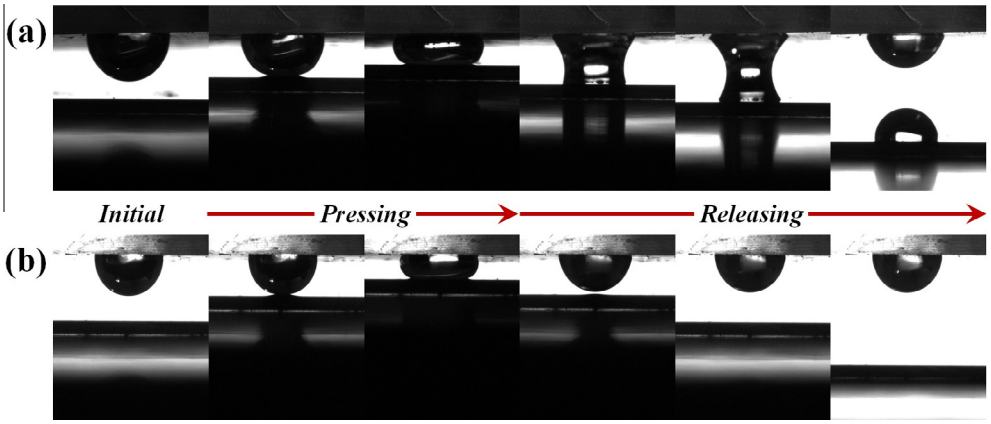

Fig. 3 – Sequential images of water droplets squeezed on (a) as-prepared and (b) silicone-coated VACNT forests. (A color version of this figure can be viewed online.)

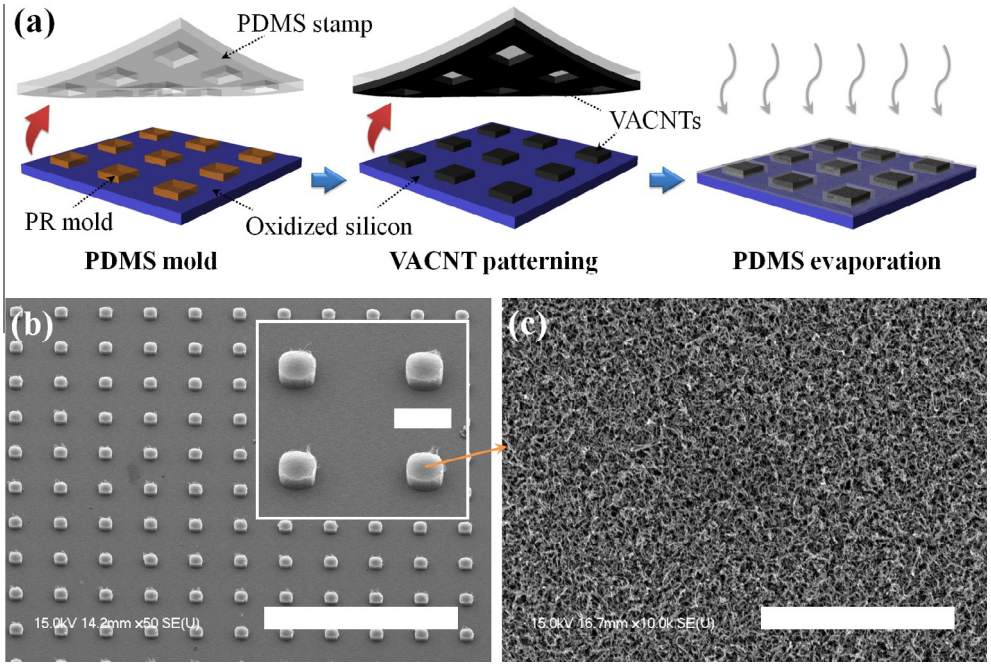

Fig. 4 – Fabrication of hierarchical VACNT superhydrophobic surfaces. (a) Schematic illustrations of key fabrication procedures. (b) SEM image of the fabricated VACNT micro-pillar arrays (scale bar: 1 mm) (inset: enlarged view of micro-pillars, scale bar: 100 μm). (c) Magnified SEM image of surface morphology of the pillar top area. (A color version of this figure can be viewed online.)

hand, the water droplet completely remained on the PDMS slab after the squeezing test, clearly showing that the silicone-coated VACNT forest is highly water-repellent, as shown in Fig. 3(b). This is due to the fact that the functional hydrophobic silicone layer is coated conformally even inside the forest, not only at the surface area, as proven by SEM and EDX investigations (Fig. S1 in Supporting Information).

Fig. 4 shows the key fabrication process of the proposed hierarchical VACNT superhydrophobic surfaces based on the facile contact transfer of VACNTs and subsequent vapor phase silicone deposition. The resultant VACNT micro-pillar-arrayed hierarchical surfaces are shown in Fig. 4(b), indicating uniform morphologies in terms of pillar widths and heights and pillar-to-pillar spacings. The magnified SEM image of the pillar top surface in Fig. 4(c) shows that the inherent nanoscale morphologies are still maintained without significant changes after the process.

Fig. 5 shows the surface wetting properties examined on the fabricated hierarchical VACNT superhydrophobic surfaces, and the performance was also summarized in Table S1 in Supporting Information. Although a high WCA of 154.7 ± 1.8° was achieved on the silicone-coated VACNT forest (nanoscale roughness), the static wetting properties were further enhanced by incorporating micro-pillar-arrayed

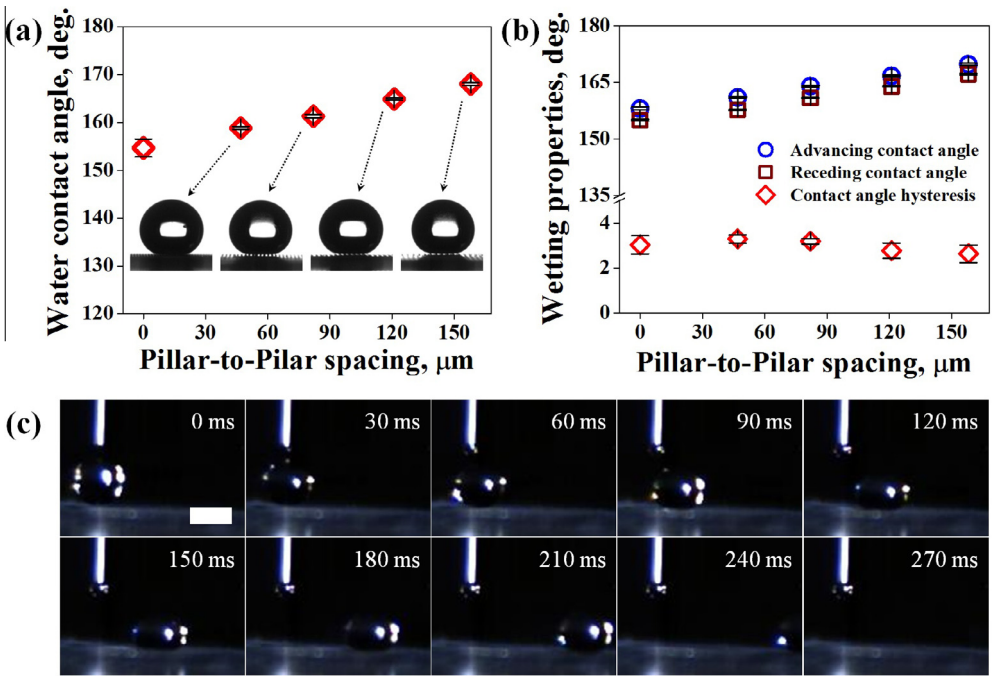

Fig. 5 – Surface wetting properties of the hierarchical VACNT superhydrophobic surfaces. (a) WCAs (inset: water droplets sitting on each surface). (b) CAHs as a function of pillar-to-pillar spacings. (c) Sequential snapshots of water droplet rolling off the hierarchical surface tilted with ~5° (scale bar: 2 mm). (A color version of this figure can be viewed online.)

morphologies (microscale roughness), as shown in Fig. 5(a). Moreover, the WCAs of the hierarchical VACNT surfaces were gradually increased by increasing the pillar-to-pillar spacing, which is consistent with Cassie-Baxter theory [34]. The highest WCA of 168 ± 0.3° was found on the surface with an inter-pillar spacing of 160 μm. This means that the micro-pillar-arrayed surface geometries provide sufficient spaces that can support water droplets, preventing the bottom surfaces from being wet. In addition, the lowest CAH of 2.64 ± 0.4° was also obtained by increasing the pillar-to-pillar spacing to 160 μm mainly due to the considerable reduction of the actual contact area of water droplets (increase in fraction of air), as shown in Fig. 5(b).

The roll-off characteristics of water droplets on the hierarchical VACNT forests were examined by the sliding test. Fig. 5(c) shows a series of snapshots of a water droplet rolling off the prepared hierarchical VACNT forest placed on the stage tilted by ~5°. After dispensing, the droplet immediately rolled off from the surface without pinning and disappeared completely within hundreds of milliseconds, as shown in Fig. 5(c). In addition, it was clearly seen that the droplet almost perfectly maintains its spherical shape when rolling off. This confirms that the difference between the advancing and receding WCAs is insignificant, which corresponds to the low hysteresis (Fig. 5(b)). This is more clear evidence that the hierarchical VACNT surfaces are in the Cassie-Baxter state.

The water-repellent characteristics of the hierarchical VACNT surfaces under dynamic conditions were evaluated by observing the impinging-and-rebounding behavior of falling water droplets. Fig. 6 shows the sequential photographs of the droplet captured every 4 ms during the dynamic impact

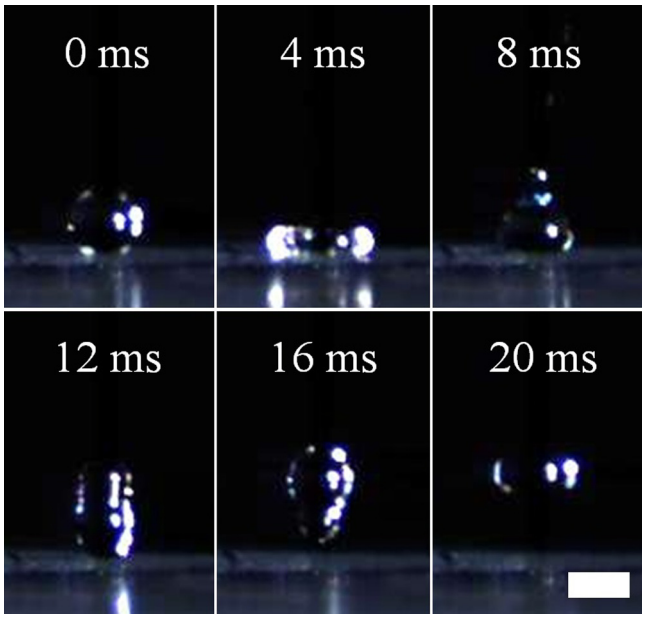

Fig. 6 – Sequential photographs of water droplet impinging on the hierarchical surface at impact velocity of ~0.63 m/s (scale bar: 2 mm). (A color version of this figure can be viewed online.)

test with an impact velocity (V_I) of ~0.63 m/s, which corresponds to the impact height of 20 mm.

The droplet impinging on the surface first spread maximally. Subsequently, the droplet started to retract, followed by perfectly rebounding from the surface without any pinning or splashing phenomena, as shown in Fig. 6. Upon

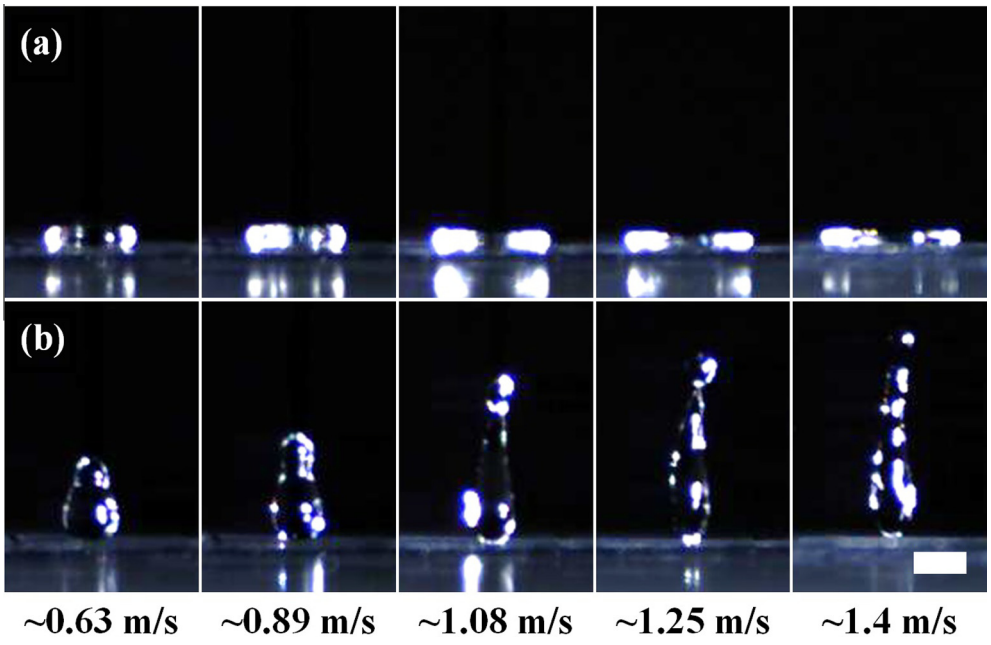

Fig. 7 – Digital images of impinging water droplets in the (a) spreading and (b) elongation (just before rebounding) stages at different impact velocities (scale bar: 2 mm). (A color version of this figure can be viewed online.)

impingement, the balance of wetting pressures (water hammer pressure (P_H) and dynamic pressure (P_D)) of impinging droplets and anti-wetting pressure (capillary pressure (P_C)) of roughened surfaces determines the surface wetting states. In particular, superior water-repellent performance can be achieved only when P_C is larger than both P_H and P_D [35–37]. The complete rebound of the droplet (at $V_I = \sim 0.63$ m/s) on the hierarchical VACNT surface reveals that the effective anti-wetting capillary pressure of the surface is high enough to entirely repel the impinging droplet.

To further examine the effect of the unique VACNT architectures on the superhydrophobic robustness of the hierarchical surfaces with respect to droplet impingement, impact tests were carried out at higher impact velocities ranging from ~0.89 to ~1.4 m/s (corresponding to impact heights of 40–100 mm). Fig. 7 shows the digital images of impinging droplets in the spreading and elongation (just before rebounding) stages at different impact velocities.

It was seen that the impinging droplets are more severely deformed in the spreading stage and subsequently lengthen out more in the elongation stage with increasing impact velocity. Nevertheless, the droplets eventually rebounded completely from the surface while retaining the superior water-repellency for all of the tested velocities, as shown in Fig. S4 in Supporting Information. This suggests that the unique architectures of the micro-pillars made of densely aligned high-aspect-ratio CNTs coated conformally with hydrophobic silicone play a significant role in achieving high effective anti-wetting capillary pressure of the micro-pillar-arrayed surface.

The experimental observations clearly suggest that the simple combination of the contact transfer and subsequent silicone coating processes makes it possible to prepare a new class of high-performance hierarchical superhydrophobic surfaces while ensuring superhydrophobic robustness in the Cassie-Baxter regime.

4. Conclusions

High-performance hierarchical superhydrophobic surfaces based on VACNT forests with inherent nanoscale roughness were demonstrated by simple contact transfer and subsequent silicone coating processes. The surface wetting properties of VACNT forests were enhanced and significantly stabilized through the conformal deposition of a thin silicone layer. The conformal deposition of the thin silicone layer was experimentally proven by SEM and EDX characterizations. Further improvement of the surface wetting properties was achieved by producing periodic VACNT micro-pillar arrays using a facile contact transfer technique. The resultant hierarchical VACNT surfaces showed superior superhydrophobicity (WCA of 168 ± 0.3°, CAH of 2.64 ± 0.4°, and sliding angle of <~5° for 160-μm-spaced sample) in the Cassie-Baxter regime. In addition, the hierarchical surfaces were found to be highly water-repellent (complete droplet rebounding at impact velocity of up to ~1.4 m/s), which is facilitated by the improved effective anti-wetting capillary pressure with the help of inherent nanoscale roughness of the VACNT micro-pillars.

Acknowledgements

This research was supported by the Basic Science Research Program (2011-0014709) and the Civil & Military Technology Cooperation Program (No. 2013M3C1A9055407) through the National Research Foundation of Korea (NRF) funded by the Ministry of Science, ICT & Future Planning.

Appendix A. Supplementary data

Supplementary data associated with this article can be found, in the online version, at http://dx.doi.org/10.1016/j.carbon.2014.08.002.

REFERENCES

[1] Yao X, Song Y, Jiang L. Applications of bio-inspired special wettable surfaces. Adv Mater 2011;23:719–34.
[2] Xue C-H, Jia S-T, Zhang J, Ma J-Z. Large-area fabrication of superhydrophobic surfaces for practical applications: an overview. Sci Technol Adv Mater 2010;11:033002.
[3] Crick CR, Parkin IP. Preparation and characterisation of superhydrophobic surfaces. Chem-Eur J 2010;16:3568–88.
[4] Guo Z, Liu W, Su B-L. Superhydrophobic surfaces: from natural to biomimetic to functional. J Colloid Interface Sci 2011;353:335–55.
[5] Li X-M, Reinhoudt D, Crego-Calama M. What do we need for a superhydrophobic surface? A review on the recent progress in the preparation of superhydrophobic surfaces. Chem Soc Rev 2007;36:1350–68.
[6] Yan YY, Gao N, Barthlott W. Mimicking natural superhydrophobic surfaces and grasping the wetting process: a review on recent progress in preparing superhydrophobic surfaces. Adv Colloid Interface Sci 2011;169:80–105.
[7] Roach P, Shirtcliffe NJ, Newton MI. Progress in superhydrophobic surface development. Soft Matter 2008;4:224–40.
[8] Huang L, Lau SP, Yang HY, Leong ESP, Yu SF, Prawer S. Stable superhydrophobic surface via carbon nanotubes coated with a ZnO thin film. J Phys Chem B 2005;109:7746–8.
[9] Lau KKS, Bico J, Teo KBK, Chhowalla M, Amaratunga GAJ, Milne WI, et al. Superhydrophobic carbon nanotube forests. Nano Lett 2003;3:1701–5.
[10] Ramos SC, Vasconcelos G, Antunes EF, Lobo AO, Trava-Airoldi VJ, Corat EJ. CO_2 laser treatment for stabilization of the superhydrophobicity of carbon nanotube surfaces. J Vac Sci Technol B 2010;28:1153–7.
[11] Journet C, Moulinet S, Ybert C, Purcell ST, Bocquet L. Contact angle measurements on superhydrophobic carbon nanotube forests: effect of fluid pressure. Eur phys Lett 2005;71:104–9.
[12] Joseph P, Cottin-Bizonne C, Benoît J-M, Ybert C, Journet C, Tabeling P, et al. Slippage of water past superhydrophobic carbon nanotube forests in microchannels. Phys Rev Lett 2006;97:156104.
[13] Li H, Wang X, Song Y, Liu Y, Li Q, Jiang L, et al. Super-"amphiphobic" aligned carbon nanotube films. Angew Chem Int Ed 2001;40:1743–6.
[14] Nosonovsky M, Bhushan B. Hierarchical roughness makes superhydrophobic states stable. Microelectron Eng 2007;84:382–6.
[15] Gao L, McCarthy TJ. The "lotus effect" explained: two reasons why two length scales of topography are important. Langmuir 2006;22:2966–7.
[16] Kwon Y, Patankar N, Choi J, Lee J. Design of surface hierarchy for extreme hydrophobicity. Langmuir 2009;25:6129–36.
[17] Kim S-J, Kim T-H, Kong J-H, Kim Y, Cho C-R, Kim S-H, et al. Dual-scale artificial lotus leaf fabricated by fully nonlithographic simple approach based on sandblasting and anodic aluminum oxidation techniques. Appl Surf Sci 2012;263:648–54.
[18] Yu E, Lee HJ, Ko T-J, Kim SJ, Lee K-R, Oh KH, et al. Hierarchical structures of AlOOH nanoflakes nested on Si nanopillars with anti-reflectance and superhydrophobicity. Nanoscale 2013;5:10014–21.
[19] Xu L, Dong LM, Li W. A simple "two foil" approach to the fabrication of hierarchical superhydrophobic surfaces. Colloids Surf A 2012;404:12–6.
[20] Maitra T, Antonini C, Mauer M, Stamatopoulos C, Tiwari MK, Poulikakos D. Hierarchically nanotextured surfaces maintaining superhydrophobicity under severely adverse conditions. Nanoscale 2014;6:8710–9.
[21] Meng Z, Yang W, Chen P, Wang W, Jia X, Xi K. Preparation of disk-like particles with micro/nano hierarchical structures. J Colloid Interface Sci 2013;408:1–5.
[22] Dai S, Zhang D, Shi Q, Han X, Wang S, Du Z. Biomimetic fabrication and tunable wetting properties of three-dimensional hierarchical ZnO structures by combining soft lithography template with lotus leaf and hydrothermal treatments. CrystEngComm 2013;15:5417–24.
[23] Tuvshindorj U, Yildirim A, Ozturk FE, Bayindir M. Robust Cassie state of wetting in transparent superhydrophobic coatings. ACS Appl Mater Interfaces 2014;6:9680–8.
[24] Hao L, Chen Z, Wang R, Guo C, Zhang P, Pang S. A non-aqueous electrodeposition process for fabrication of superhydrophobic surface with hierarchical micro/nano structure. Appl Surf Sci 2012;258:8970–3.
[25] Sun T, Wang G, Liu H, Feng L, Jiang L, Zhu D. Control over the wettability of an aligned carbon nanotube film. J Am Chem Soc 2003;125:14996–7.
[26] Chen L, Xiao Z, Chan PCH, Lee Y-K. Static and dynamic characterization of robust superhydrophobic surfaces built from nano-flowers on silicon micro-post arrays. J Micromech Microeng 2010;20:105001.
[27] Zhu L, Xiu Y, Xu J, Tamirisa PA, Hess DW, Wong C-P. Superhydrophobicity on two-tier rough surfaces fabricated by controlled growth of aligned carbon nanotube arrays coated with fluorocarbon. Langmuir 2005;21:11208–12.
[28] Sethi S, Ge L, Ci L, Ajayan PM, Dhinojwala A. Gecko-inspired carbon nanotube-based self-cleaning adhesives. Nano Lett 2008;8:822–5.
[29] Zhang L, Resasco DE. Single-walled carbon nanotube pillars: a superhydrophobic surface. Langmuir 2009;25:4792–8.
[30] Huang J-Q, Zhang Q, Zhao M-Q, Xu G-H, Wei F. Patterning of hydrophobic three-dimensional carbon nanotube architectures by a pattern transfer approach. Nanoscale 2010;2:1401–4.
[31] Jeong G-H, Olofssona N, Falkc LKL, Campbell EEB. Effect of catalyst pattern geometry on the growth of vertically aligned carbon nanotube arrays. Carbon 2009;47:696–704.
[32] Lu SH, Tun MHN, Mei ZJ, Chia GH, Lim X, Sow C-H. Improved hydrophobicity of carbon nanotube arrays with micropatterning. Langmuir 2009;25:12806–11.
[33] Yuan JK, Liu XG, Akbulut O, Hu JQ, Suib SL, Kong J, et al. Superwetting nanowire membranes for selective absorption. Nat Nanotechnol 2008;3:332–6.
[34] Cassie ABD, Baxter S. Wettability of porous surfaces. Trans Faraday Soc 1944;40:546–51.
[35] Kwon H-M, Paxson AT, Varanasi KK, Patankar NA. Rapid deceleration-driven wetting transition during pendant drop deposition on superhydrophobic surface. Phys Rev Lett 2011;106:036102.
[36] Kwon DH, Lee SJ. Impact and wetting behavior of impinging microdroplets on superhydrophobic textured surfaces. Appl Phys Lett 2012;100:171601.
[37] McCarthy M, Gerasopoulos K, Enright R, Culver JN, Chodssi R, Wang EN. Biotemplated hierarchical surfaces and the role of dual length scales on the repellency of impacting droplets. Appl Phys Lett 2012;100:263701.